Polarforschung 67 (1/2), 77 – 86, 1997 (erschienen 2000)

Ice-Sheet Geometry in Western Neuschwabenland, Antarctica

By Henner Sandhäger[1] and Norbert Blindow[1]

Summary: Extensive aero-geophysical measurements (altimetry, radio-echo sounding), carried out between 1985 and 1989 by the Institut für Geophysik der Universität Münster, yield new maps of ice-surface elevation, ice thickness, and subglacial-bedrock topography for western Neuschwabenland. This East Antarctic ice-sheet region adjoins to the Atlantic Ocean and covers an area of about 325,000 km². The maps depict geometric characteristics of three zones: the coastal strip including different ice shelves and ice rises; the grounded ice masses of Ritscherflya adjacent to the south; and the northern margin of the East Antarctic plateau located south of the Heimefrontfjella mountain range. In particular, the subglacial-bedrock relief of Ritscherflya is resolved in detail. Its southwestern part is dominated by a large depression with depths up to ~1000 m below sea level and ice thicknesses exceeding 1800 m, while the bedrock in the central part steadily rises inland from the grounding line. The northeastern part of Ritscherflya includes prominent ice covered mountainous areas. Furthermore, several graben-like depressions in the bedrock topography become evident, which are likely connected with zones of concentrated ice flux from inland into the ice shelves. The most distinct of these structures coincides with the boundaries of the outlet glacier Jutulstraumen draining into the ice shelf Fimbulisen. The new geometric data sets also represent an outstanding base for future studies such as on ice dynamics or tectonics.

Zusammenfassung: Anhand umfangreicher Flugmessungen (Altimetrie und Registrierungen mit dem elektromagnetischen Reflexionsverfahren), die das Institut für Geophysik der Universität Münster zwischen 1985 und 1989 durchführte, wurden neue Karten der Höhe der Eisoberseite, der Eismächtigkeit und der subglazialen Felsbettopographie für das westliche Neuschwabenland erstellt. Dieses umfasst einen etwa 325.000 km² großen Randbereich des ostantarktischen Eisschildes und grenzt direkt an den Atlantik. Die Karten zeigen Merkmale der Eiskörpergeometrie in drei Regionen: im Küstenstreifen mit den verschiedenen Schelfeisen und Eiskuppeln, im südlich angrenzenden Inlandeisbereich Ritscherflya und in der nördlichen Randzone des ostantarktischen Plateaus, die südlich der Gebirgskette Heimefrontfjella liegt. Insbesondere ist das Relief des Felsbettes im Bereich Ritscherflya detailliert erfasst. Während der südwestliche Teil durch eine ausgedehnte Senke geprägt ist, die bis zu ~1000 m unter das Meeresniveau hinabreicht und mit über 1800 m mächtigem Eis gefüllt ist, steigt der subglaziale Felsuntergrund im Zentralteil von der Aufsetzlinie in Richtung Inland relativ gleichmäßig an. Im nordöstlichen Teil der Ritscherflya treten ausgeprägte eisbedeckte Gebirgsstrukturen auf. Weiterhin sind mehrere grabenförmige Senken in der Felsbettopographie aufgelöst, die wahrscheinlich mit Hauptabflussbereichen von Inlandeismassen in die vorgelagerten Schelfeise zusammenfallen. Die bedeutendste dieser Strukturen ist der Auslassgletscher Jutulstraumen, der in das Schelfeis Fimbulisen mündet. Die neuen digitalen geometrischen Modelle stellen somit eine wesentliche Grundlage für zukünftige Untersuchungen z.B. zur Eisdynamik oder Tektonik dar.

INTRODUCTION

Western Neuschwabenland is a coastal region of the East Antarctic Ice Sheet and extends from about 0° to 15 °W and from about 70 °S to 76 °S (Fig. 1). Covering an area of ~325,000 km² and bordering directly on the Atlantic Ocean, it includes several comparatively small drainage systems (Drewry 1983) such as the ice shelves Riiser-Larsenisen, Quarisen, Ekströmisen, Jelbartisen, and Fimbulisen together with their accompanying catchment areas (BKG 1998). Besides the flat ice shelves and the grounded ice domes in between, another significant topographic feature of western Neuschwabenland is a prominent mountain range, which is ~600 km long and orientated approximately from southwest to northeast at a distance between ~250 km and ~350 km inland from the ice front. Parts of this zone with numerous ice-free rock outcrops are Heimefrontfjella, Kirwanveggen, Borgmassivet, and H.U. Sverdrupfjella, the latter being separated by the outlet glacier Jutulstraumen draining into the ice shelf Fimbulisen (cf. IfAG 1993). The mountain range represents the boundary between the ice-sheet region Amundsenisen adjacent to the southeast, which belongs to the East Antarctic plateau and shows surface elevations higher than 2000 m above sea level (Drewry 1983), and the grounded ice masses of Ritscherflya adjacent to the northwest, whose eastern part Giæverryggen is characterized by prominent subglacial mountainous structures (Hoppe & Thyssen 1988, Sandhäger & Blindow 2000).

During the field season 1988/89 the Institut für Geophysik der Universität Münster carried out 22 measuring flights over western Neuschwabenland. In particular, altimetry and airborne radio-echo sounding (RES) were used on ~25,000 km of flight tracks to determine the ice-sheet geometry in this region. Together with the data recorded in 1985/86 on ~6000 km of flight tracks (Hoppe & Thyssen 1988) a sufficiently dense data coverage has been attained in the investigated area except for the regions of northern Giæverryggen and Kirwanveggen (cf. inset map of Fig. 1).

The processing of the combined data sets yields new maps showing the ice-surface topography, the ice-thickness distribution, and the subglacial-bedrock topography in western Neuschwabenland. Besides these maps, three characteristic vertical cross sections are also discussed in the following. The measurements recorded on the dense flight track pattern over the ice shelf Ekströmisen and its catchment area have been further analysed with special regard to the ice-dynamic characteristics and the mass budget of this drainage system (Sandhäger & Blindow 2000).

PROCESSING OF THE AERIAL MEASUREMENTS

The geographical positions of the measuring points along the flight tracks from the field seasons 1985/86 and 1988/89 and the

[1] Institut für Geophysik der Westfälischen Wilhelms-Universität Münster, Corrensstraße 24, D-48149 Münster, Germany

Manuscript received 18 June 1999, accepted 03 March 2000

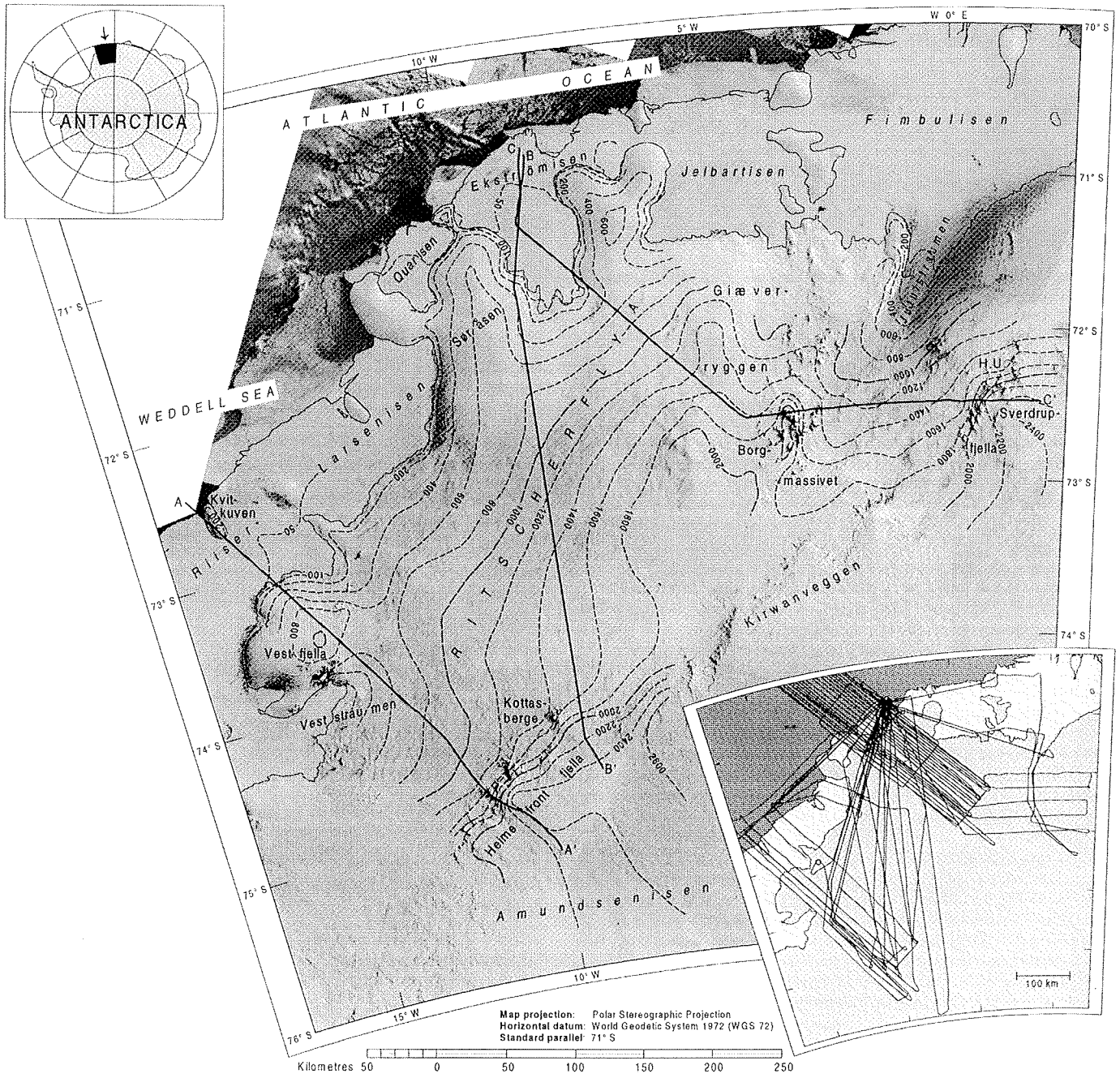

Fig. 1: Satellite-image map of western Neuschwabenland (BKG 1998) with contour lines of ice-surface elevation (in metres a.s.l.) derived from aerial measurements. The pattern of the flight tracks from the field seasons 1985/86 and 1988/89 is shown in the inset map. Here and on Figures 6 and 7, the positions of the profiles A-A', B-B', and C-C' (cf. Fig. 2) are indicated by bold lines; grounding lines and the ice front (BAS 1993) are emphasized by thin lines.

Abb. 1: Satellitenbildkarte des westlichen Neuschwabenlandes (BKG 1998) mit Höhenlinien der Eisoberseite (in Metern über Meeresniveau), die aus Flugmessdaten abgeleitet sind. Die Einlegekarte zeigt die Verläufe der 1985/86 und 1988/89 durchgeführten Messflüge. Die Lage der Profile A-A', B-B' und C-C' (vgl. Abb. 2) ist hier und in den Abbildungen 6 und 7 mit dicken Linien, die der Aufsetzlinien und der Eisfront (BAS 1993) mit dünnen Linien gekennzeichnet.

accompanying ice-surface elevations were derived from the corrected navigational and altimetry data, respectively. Errors in the navigational data resulted mainly from an irregular instrument drift. They were considerably reduced by applying a correlation procedure based on prominent topographic features, whose geographical positions were well-known from satellite-image analyses (IfAG/AWI 1994), and which also could be identified in the altimetry data and/or the RES records (cf. SANDHÄGER & BLINDOW 2000). Nevertheless, the remaining mean location error of the track data is still about ±5 km. The correction of errors in the flight-altimetry data recorded with barometric and radar altimeters was performed by aligning the data at cross-over points of flight tracks, by considering buoyancy arguments in ice-shelf areas (cf. THYSSEN & GROSFELD 1988), and by using other reliable altitude measurements (e.g. geodetic ground levelling) as reference values.

From the acquired RES records the travel-time differences of

the electromagnetic wave trains reflected from the surface and the bottom of the ice were determined and converted to ice thicknesses using a velocity-depth function which had been derived from ground-based RES near the ice front of western Ekströmisen (BLINDOW 1986). Subglacial-bedrock elevations were calculated as the difference between ice-surface elevations and ice thicknesses.

The combination of the fully processed data then yielded a final data set describing the ice-sheet and ice-shelf geometries along the flight tracks. Figure 2 shows three representative vertical cross sections based on this data set. The positions of the corresponding flight tracks are marked in Figures 1, 6, and 7. The intrinsic consistency of the final geometric data set can be assessed from Figure 3 which shows the frequency

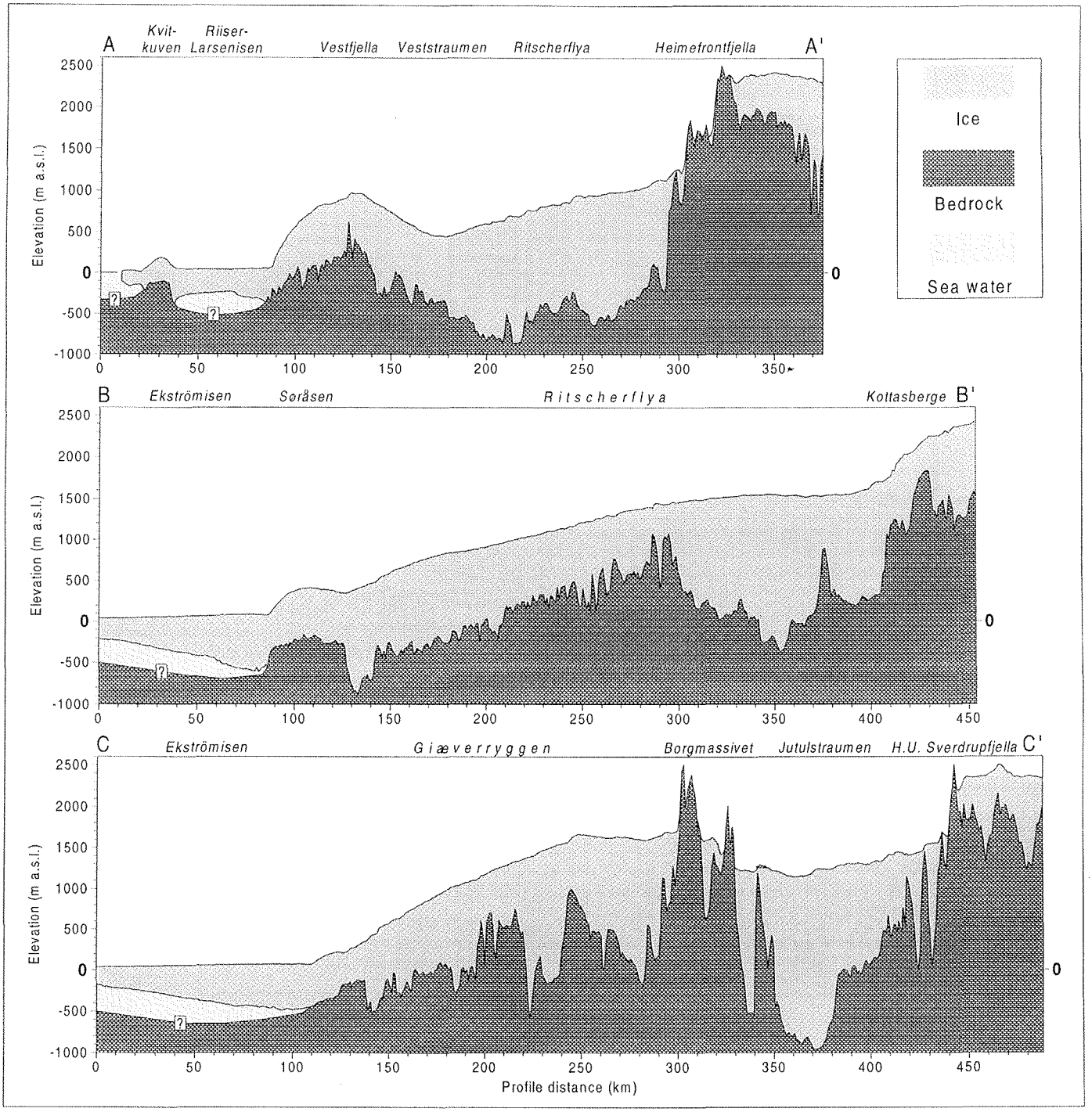

Fig. 2: Vertical cross-sections of different ice-sheet and ice-shelf regions of western Neuschwabenland. The positions of the profiles A-A', B-B', and C-C' along selected flight tracks are indicated in the maps of Figures 1, 6, and 7. The seabed topography is not determinable with RES surveys. The vertical exaggeration of the cross sections is 43:1.

Abb. 2: Profilschnitte durch den Eiskörper im westlichen Neuschwabenland. Die Lage der Profile A-A', B-B' und C-C', die entlang von Fluglinien verlaufen, ist in den Karten der Abbildungen 1, 6 und 7 markiert. Die Meeresbodentopographie kann mit dem eingesetzten elektromagnetischen Reflexionsverfahren nicht erfasst werden. Die Überhöhung der Profilschnitte beträgt 43:1.

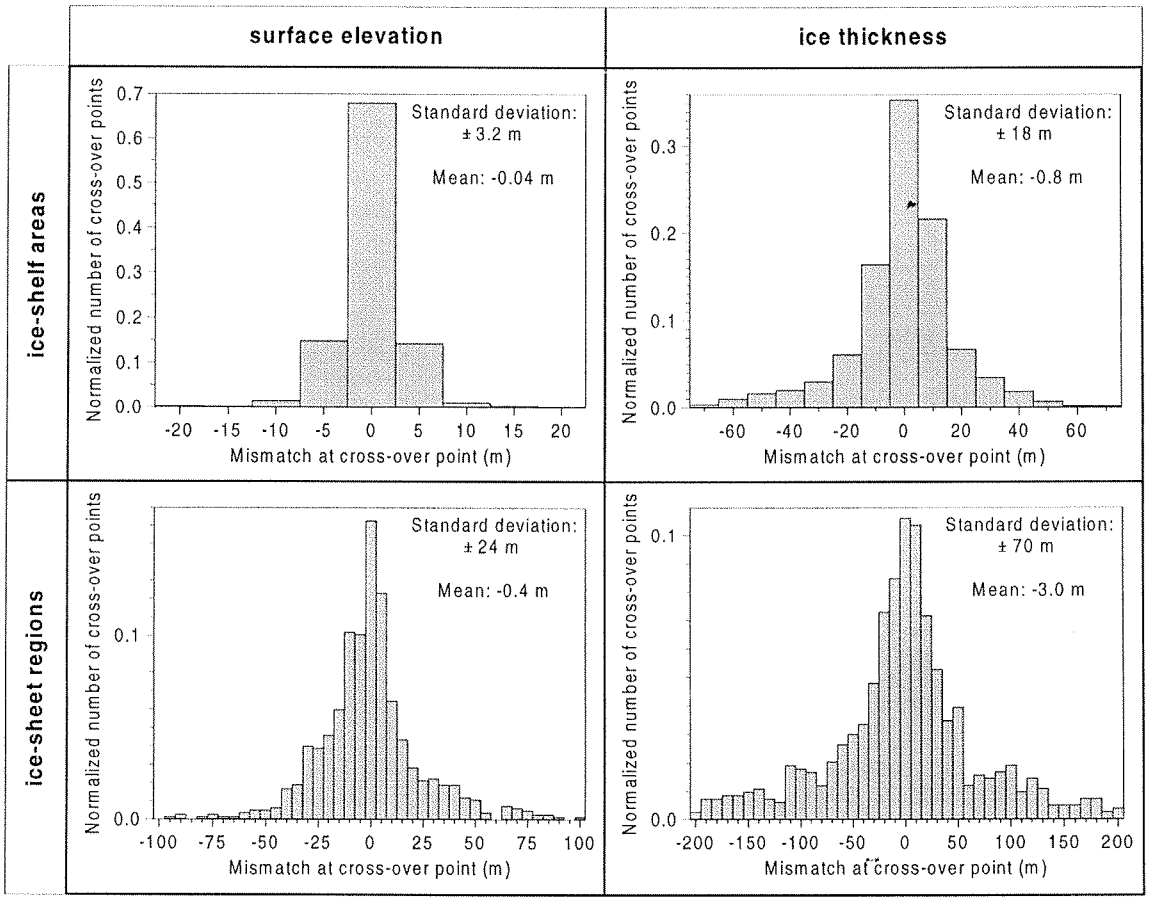

Fig. 3: Frequency distributions and statistical parameters of the mismatches of the surface-elevation and ice-thickness data acquired in close vicinities of the cross-over points of the flight tracks. The number of considered measuring points located in ice-shelf and ice-sheet regions is about 2500 and 1500, respectively. Elevation and thickness mismatches were grouped into 5 m and 10 m bins, respectively.

Abb. 3: Häufigkeitsverteilungen und statistische Kenngrößen der Abweichungen in den Oberflächenhöhen- und Eismächtigkeitswerten aus den Nahbereichen der Kreuzungspunkte der Flugprofile. Berücksichtigt sind etwa 2500 Messpunkte in Schelfeisgebieten und etwa 1500 Messpunkte in Inlandeisregionen. Die Höhendifferenzen wurden 5 m-Intervallen, die Mächtigkeitsdifferenzen 10 m-Intervallen zugeordnet.

distributions and statistical parameters of the mismatches of the surface-elevation and ice-thickness data acquired in close vicinities of the cross-over points of the flight tracks. In particular, the resulting standard deviations of both ice-surface elevation and ice thickness are found to be considerably larger in the investigated ice-sheet regions than in the marginal ice-shelf areas. This is a direct consequence of the much more uniform surface topographies and ice-thickness distributions of most of the floating ice-shelf portions. The accompanying standard deviations of ±3.2 m (surface elevation) and ±18 m (ice thickness) therefore represent lower limiting values of the error tolerances for the ice-shelf geometry as quantified from the aerial measurements (cf. Tab. 1).

To derive digital geometric models, which describe the ice-surface and subglacial-bedrock topographies and the ice-thickness distribution in the whole investigated region, the measuring points of the geometric quantities along the flight tracks were interpolated on regular horizontal grids. For this, a geostatistical gridding method was used which attempts to express trends that are suggested in the source data. Depending on the local density of the measuring points and on the actual selection of the interpolation-algorithm parameters, several parts of the resulting digital models only provide a strongly smoothed or even distorted image of the real geometric setting in the corresponding ice-sheet regions. A significant reduction of these inaccuracies has been achieved by a manual post-processing especially of those parts of the geometric models representing areas where prominent subglacial mountainous structures and/or ice-free mountain outcrops cause differences in ice thickness and bedrock elevation of partly more than 1000 m on horizontal distances of only a few kilometres (cf. Fig. 2). The estimated local error tolerances for the geometric quantities in the corresponding final digital models are summarised in Table 1. The magnitudes of these error tolerances are largely confirmed in the surface-elevation and ice-thickness differences shown in Figure 4. They occur when the ice-body geometry along the flight-track section B-B' (cf. Fig. 2) is determined either directly from the measurements or by interpolation from the digital terrain and ice-thickness models, respectively.

	surface elevation	ice thickness	bedrock elevation
ice-shelf areas	±5 m – ±10 m	±15 m – ±75 m	–
ice-sheet regions (A)	±10 m – ±50 m	±25 m – ±100 m	±30 m – ±110 m
ice-sheet regions (B) [particular ice-sheet regions (B) with prominent subglacial mountainous structures and/or ice-free mountain outcrops]	±50 m – ±200 m [±1000 m]	±100 m – ±250 m [±2000 m]	±110 m – ±320 m [±2250 m]

Tab. 1: Error tolerances for the three geometric quantities in the corresponding digital models which form the basis of the contour maps shown in Figures 1, 6, and 7. In ice-sheet regions (A) the number of measuring points is comparatively large and/or the horizontal gradients of the relevant geometric quantity are small. Ice-sheet regions (B) are characterized by a sparse covering of measuring points and/or relatively large lateral variations in ice-sheet geometry.

Tab. 1: Fehlertoleranzen für die drei geometrischen Größen in den entsprechenden digitalen Modellen, die den in den Abbildungen 1, 6 und 7 dargestellten Isolinienkarten zugrunde liegen. In Eisschildbereichen (A) ist die Anzahl der Messpunkte vergleichsweise groß, und/oder die Horizontalgradienten der jeweiligen geometrischen Größe sind klein. Eisschildbereiche (B) sind durch eine geringe Messpunktdichte und/oder relativ große laterale Änderungen der Eiskörpergeometrie gekennzeichnet.

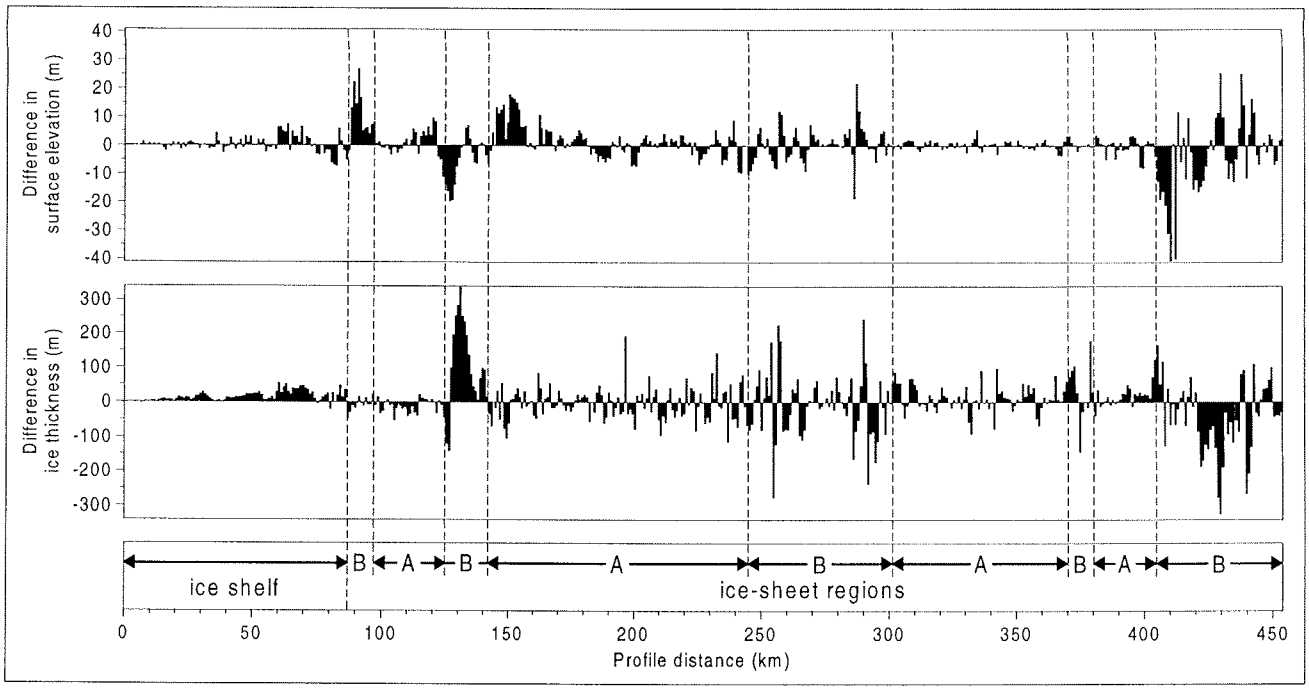

Fig. 4: Surface-elevation and ice-thickness differences along the flight-track section B-B' (cf. Fig. 1 and 2) which occur when the ice-body geometry is determined either directly from the measurements or by interpolation from the digital terrain and ice-thickness models, respectively. Large discrepancies mainly arise in the ice-sheet regions B where the horizontal gradients of the different geometric quantities are considerably larger than in the ice-sheet regions A and in the ice-shelf area.

Abb. 4: Höhen- und Eismächtigkeitsdifferenzen entlang des Flugprofils B-B' (vgl. Abb. 1 und 2), die auftreten, wenn die Eiskörpergeometrie entweder direkt anhand der Messwerte oder durch Interpolation anhand des digitalen Gelände- und Eisdickenmodells bestimmt wird. Große Abweichungen ergeben sich vor allem in den Inlandeisregionen B, wo die Horizontalgradienten der verschiedenen geometrischen Größen erheblich ausgeprägter sind als in den Inlandeisregionen A und im Schelfeisbereich.

ICE-SURFACE TOPOGRAPHY

From the digital terrain model of western Neuschwabenland a new topographic map has been derived which is shown in Figure 1. The contour lines of ice-surface elevation overlay a satellite-image mosaic (BKG 1998) and are plotted at intervals of 200 m. The 50 m- and 100 m-contour lines are added where appropriate.

With increasing distance from the coast the ice surface generally rises towards the southeast from less than 100 m above sea level in the ice-shelf areas and grounding zones to more than 2500 m in the northern part of the ice-sheet region Amundsenisen. The mean surface slope, however, changes from ~10 m km^{-1} in the area of Ritscherflya to 20 m km^{-1} up to 45 m km^{-1} in the mountain range adjacent to the southeast. Further inland the surface gradient decreases again and is ~5 m km^{-1} on average

in northern Amundsenisen. These significant lateral variations in the surface slope, also visible in the vertical cross sections A-A' and B-B' (Fig. 2), show that the mountain range between Ritscherflya and Amundsenisen constitutes a prominent step in the surface relief of western Neuschwabenland and prevents an uniformly distributed ice flux from the central East Antarctic plateau into the coastal zone. In addition, the mountain range probably has a repressive effect on the ice masses grounded further to the southeast and thereby contributes to the stabilisation of the East Antarctic Ice Sheet.

The mass discharge from Amundsenisen into Ritscherflya and the adjacent ice shelves is mainly concentrated on several outlet glaciers cutting through the mountain range. The most distinct outlet glacier within the investigated area is Jutulstraumen which is bounded by the mountainous regions Borgmassivet and H.U. Sverdrupfjella to the west and east, respectively (cf. cross section C-C' in Fig. 2), and drains into the ice shelf Fimbulisen. The entire catchment area of Jutulstraumen extends over a ~100,000 km² large area of northern Amundsenisen (Drewry 1983, BKG 1998). The steady increase of the surface slope of Jutulstraumen between its upper reaches (about -8 m km^{-1}) and its grounding zone (about -18 m km^{-1}) emphasizes that also the velocity of the glacier flow considerably increases downstream.

The surface topography in the northeastern part of Ritscherflya is characterized by various large-scale surface undulations which mainly appear in the area of Giæverryggen and laterally extend over several tens of kilometres. The distinctive shape of the ice surface clearly reflects the strong influence of the prominent subglacial mountainous structures on the motion of the ice masses grounded in this region (cf. cross section C-C' in Fig. 2). In contrast, the ice-surface relief in the central and southwestern parts of Ritscherflya is relatively smooth apart from slight small-scale undulations. This points to a considerably more uniform flow regime according to the comparatively even subglacial-bedrock topography mainly structured by small-scale bedrock undulations there (cf. cross sections A-A' and B-B' in Fig. 2).

The three largest of the dome-shaped ice caps, which border on Ritscherflya in the north and separate the different ice shelves from each other, are Vestfjella, Søråsen, and Halvfarryggen. Søråsen is crowned by a 50 km long crest at altitudes between 725 m and 750 m (cf. Sandhäger & Blindow 2000), while each of the ice domes Vestfjella and Halvfarryggen includes a prominent summit rising to about 1000 m and 675 m above sea level, respectively. The flow regimes of the ice domes are largely independent of the ice movement in the Ritscherflya region.

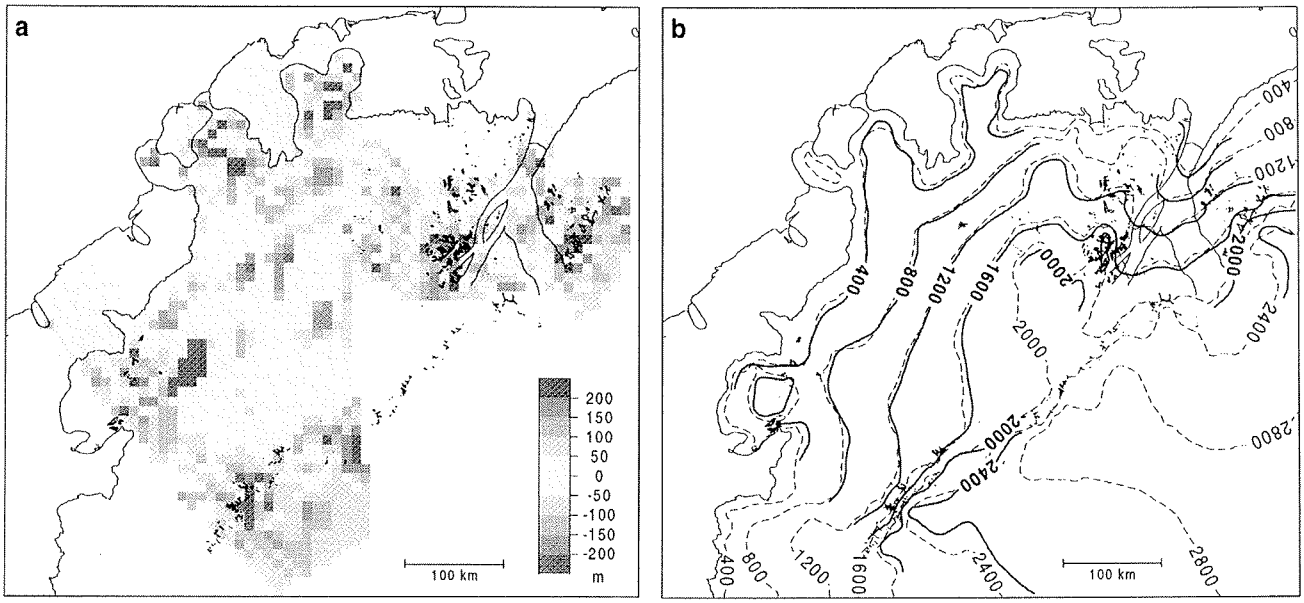

Fig. 5: **(a)** Discrepancies between the new digital elevation model derived from the aerial measurements and a digital terrain model determined by Bamber & Huybrechts (1996) mainly from satellite-altimetry data. Elevation differences were calculated at the relevant grid points of the latter model. According to its horizontal resolution of 10 km, each of the resulting values was assigned to an area covering 100 km² and being emphasized in the map by the accompanying grey colour filling. **(b)** Comparison between selected surface-elevation contours (in m) which were derived from the new digital elevation model (bold lines) and extracted from a satellite-image map of Dronning Maud Land (BKG 1998; dashed lines), respectively. The latter represent an edited set of contour lines originating from the digital terrain model developed by Bamber & Huybrechts (1996). (Base map from BAS 1993, IfAG/AWI 1994, BKG 1998)

Abb. 5: **(a)** Abweichungen zwischen dem neuen, aus Flugmessdaten abgeleiteten digitalen Höhenmodell und einem von Bamber & Huybrechts (1996) ermittelten digitalen Geländemodell, das vor allem auf Satellitenaltimetriedaten basiert. Höhendifferenzen wurden an den relevanten Gitterpunkten des zweiten Modells berechnet. Entsprechend dessen horizontaler Auflösung von 10 km wurde jeder so bestimmte Differenzwert einem 100 km² großen Gebiet zugeordnet, das in der Karte mit der jeweils zugehörige Grauschattierung gekennzeichnet ist. **(b)** Vergleich zwischen ausgewählten Höhenlinien (in m), die aus dem neuen digitalen Höhenmodell abgeleitet (dicke Linien) bzw. einer Satellitenbildkarte des Dronning Maud Landes (BKG, 1998) entnommen wurden (gestrichelte Linien). Letztere stellen eine nachbearbeitete Version derjenigen Höhenlinien dar, die direkt aus dem von Bamber & Huybrechts (1996) entwickelten digitalen Geländemodell hervorgehen. (Kartenbasis: BAS 1993, IfAG/AWI 1994, BKG 1998)

A comparison between the new digital terrain model, derived from flight altimetry data, and the pattern of surface-elevation contours presented by DREWRY (1983) yields local discrepancies in the determined altitudes of up to ±400 m, resulting most likely from the large difference in the number of altitude measurements on which each of the terrain models is based. In contrast to that, there are considerably smaller discrepancies between the new surface-elevation model and the digital terrain model developed by BAMBER & HUYBRECHTS (1996) mainly on the basis of satellite-altimetry data (Fig. 5a). The surface-elevation differences are less than ±50 m (±100 m) at about 55 % (80 %) of the common grid points within the investigation area, but also exceed ±200 m at several grid points located partly in ice-sheet regions with prominent subglacial mountainous structures and/or ice-free mountain outcrops and partly in other ice-sheet areas. However, an overall good agreement is found between the new surface-elevation contours (Fig. 1) and an edited set of contour lines (extracted from BKG 1998) originating from the digital terrain model derived by BAMBER & HUYBRECHTS (1996). Figure

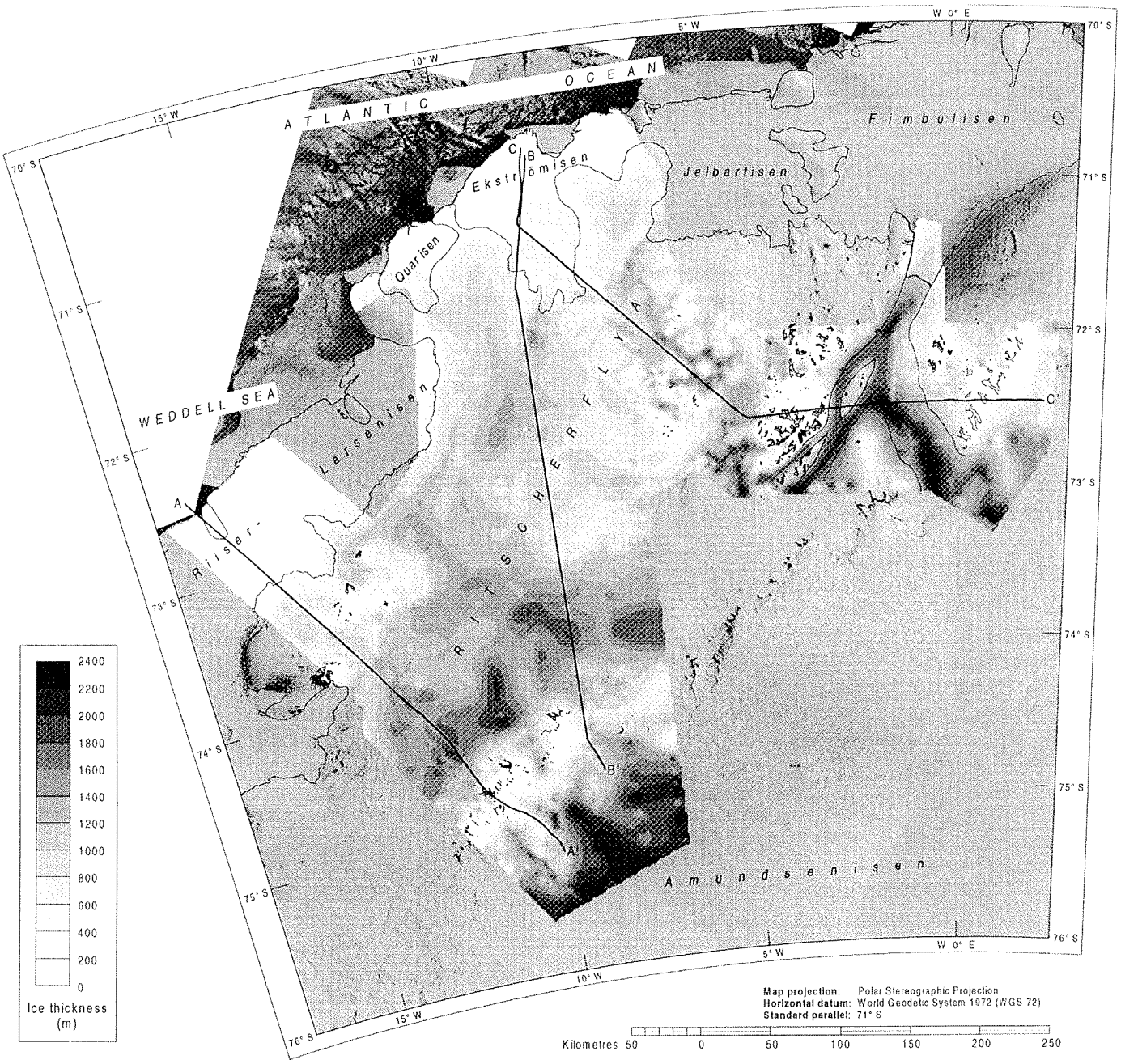

Fig. 6: Ice-thickness distribution in western Neuschwabenland. The basic digital ice-thickness model has been derived from airborne RES data recorded in 1985/86 and 1988/89. Areas between the contours of ice thickness are filled with gradated grey colours and are plotted on a satellite-image mosaic (BKG 1998). Ice-free rock outcrops and striking mountainous structures (extracted from BAS 1993, IfAG/AWI 1994, BKG 1998) are emphasized by thin black lines.

Abb. 6: Eismächtigkeitsverteilung im westlichen Neuschwabenland. Das zugrundeliegende digitale Mächtigkeitsmodell ist aus Flugmessdaten abgeleitet, die 1985/86 und 1988/89 mit dem elektromagnetischen Reflexionssystem registriert wurden. Bereiche zwischen den Isolinien der Eismächtigkeit sind graustufenkodiert dargestellt und einem Satellitenbildmosaik (BKG 1998) überlagert. Eisfreie Berggipfel und hervortretende Gebirgsstrukturen (nach BAS 1993, IfAG/AWI 1994, BKG 1998) sind durch dünne schwarze Linien hervorgehoben.

5b shows a map on which the elevation contours from both sources were plotted at intervals of 400 m. The estimated mean and maximum deviations in surface elevation of about ±25 m and ±200 m, respectively, largely coincide with the corresponding error tolerances given in Table 1.

ICE-THICKNESS DISTRIBUTION

The map displayed in Figure 6 shows the ice-thickness distribution in those parts of western Neuschwabenland where the airborne RES database has been suitable to derive a digital ice-thickness model. In the map, the areas between the contours of ice thickness are filled with gradated grey colours and are plotted on a satellite-image mosaic (BKG 1998).

The largest ice thicknesses recorded within the investigated area occur along the outlet glacier Jutulstraumen and in the northern part of Amundsenisen. The thickness of the grounded ice masses partly exceeds 2000 m there. In contrast to that, the prominent mountain range, which separates the Amundsenisen and Ritscherflya regions and forms the western and eastern boundaries of Jutulstraumen, is covered by a relatively thin ice layer (mostly <400 m) penetrated by several ice-free rock outcrops (cf. cross sections in Fig. 2). Thus, also the ice-thickness map reflects the repressive effect of the mountain range on the movement of the ice masses of Amundsenisen as well as the outstanding importance of Jutulstraumen as a particular zone of concentrated ice flux from inland into the coastal area.

The ice-thickness map (Fig. 6) and the selected cross sections (Fig. 2) show that the Ritscherflya ice-sheet region can be subdivided into three main parts on the basis of the ice-thickness distribution there. The southwestern part of Ritscherflya, which extends from the ice dome Vestfjella in the northwest up to the Heimefrontfjella mountain range in the southeast, is characterized by a comparatively large mean ice thickness of ~1200 m and maximum thicknesses of more than 1800 m in places. The ice masses grounded in the central part of Ritscherflya are clearly distinguished by a considerably reduced mean thickness of just ~800 m. In the eastern part of Ritscherflya the thickness of the ice body shows large lateral variations due to the prominent subglacial mountainous structures particularly in the area of Giæverryggen. Here, several depressions in the subglacial-bedrock topography are filled with ice up to 1800 m thick, whereas in the immediate vicinity the bedrock partly rises up as far as close under the ice surface or even penetrates the ice cover.

The thickness of the floating ice shelves along the seaward margin of Ritscherflya steadily decreases from more than 800 m at several grounding-line sections to less than 200 m at the ice-shelf fronts. This characteristic thinning of the ice shelves directly results from the general increase in the velocity of the ice-shelf flow with decreasing distance from the ice fronts. Figures 2 and 6 additionally reflect the influence of the lateral topography and the ice rises and ice rumples on the flow regimes and the ice-thickness distributions of Ekströmisen and central Riiser-Larsenisen.

SUBGLACIAL-BEDROCK TOPOGRAPHY

The new subglacial-bedrock topography map of western Neuschwabenland is shown in Figure 7. Areas between the contours of bedrock elevation are filled with gradated grey colours and are plotted on a satellite-image mosaic (BKG 1998) again.

In large parts of the Ritscherflya ice-sheet region the surface of the subglacial bedrock generally declines towards the north or northeast from more than 2000 m above sea level in the southern mountain range to partly less than -600 m or -800 m in the coastal area. Along the grounding line the ice masses become afloat and contribute to the formation of the different ice shelves. Their stability is ensured by the lateral coupling to the grounded ice sheet in bays and to the ice rises and ice rumples resting on shoals within or at the seaward edge of the floating portions of the ice body. Zones of concentrated ice flux from Ritscherflya into the ice shelves usually coincide with graben-like depressions in the ice-sheet base. Some of these structures, which often extend over several tens of kilometres inland from the grounding line (cf. Sandhäger & Blindow 2000), can be clearly identified in the bedrock-topography map (Fig. 7). The most striking system composed of different connected graben-like depressions in the subglacial-bedrock relief correlates with the boundaries of the outlet glacier Jutulstraumen. The deepest parts of the glacier base are situated more than 1500 m below sea level (cf. cross section C-C' in Fig. 2).

In accordance with the ice-thickness map, also the map of subglacial-bedrock topography displayed in Figure 7 points to a general subdivision of Ritscherflya into three main parts. Although the ice dome Vestfjella is grounded on a comparatively rough bedrock surface rising up regionally to several hundreds of metres above sea level, the subglacial-bedrock surface is below sea level nearly in the whole southwestern part of Ritscherflya. The mean depth of the ice/bedrock interface is about -400 m, while maximum depths of more than -1000 m are reached in the area of some bedrock depressions. The transition to the Heimefrontfjella mountain range adjoining to the south is constituted by an abrupt change in the slope of the bedrock surface which partly ascends up to 70 m km^{-1} there (cf. cross section A-A' in Fig. 2). In contrast, the surface slope of the ice-sheet base seems to be much more smaller in the transition zone between the Kirwanveggen mountain range and the southern central part of Ritscherflya, where the bedrock surface remains above sea level in the whole area south of about 72 °S to 73 °S. The subglacial-bedrock relief in the northeastern part of Ritscherflya is mainly characterized by the prominent mountainous structures of Giæverryggen which lead to a distinct roughness of the ice-sheet base on a horizontal scale of several kilometres (cf. cross section C-C' in Fig. 2).

Compared to the bedrock-elevation map derived by Hoppe &

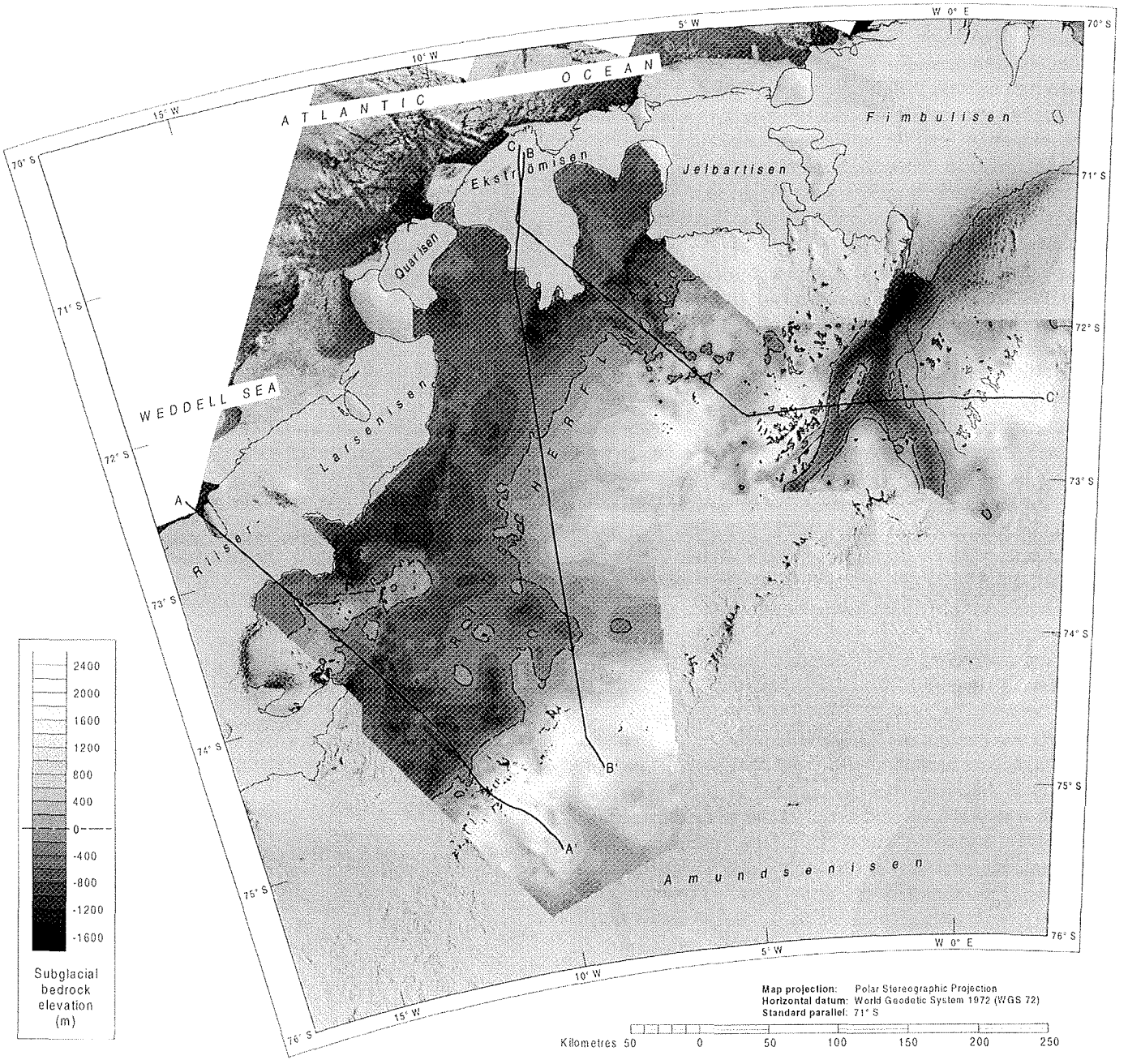

Fig. 7: Subglacial-bedrock topography in western Neuschwabenland. The basic digital bedrock-elevation model has been derived from airborne measurements carried out in 1985/86 and 1988/89. Areas between the contours of bedrock elevation (in m a.s.l.) are filled with gradated grey colours and are plotted on a satellite-image mosaic (BKG 1998). Ice-free rock outcrops and striking mountainous structures (extracted from BAS 1993, IfAG/AWI 1994, BKG 1998) are emphasized by thin black lines. The seabed topography is not derivable from the airborne measurements.

Abb. 7: Topographie des subglazialen Felsuntergrundes im westlichen Neuschwabenland. Das zugrundeliegende digitale Höhenmodell ist aus 1985/86 und 1988/89 registrierten Flugmessdaten abgeleitet. Bereiche zwischen den Isolinien der Felsbetthöhe (in m über Meeresniveau) sind graustufenkodiert dargestellt und einem Satellitenbildmosaik (BKG 1998) überlagert. Eisfreie Berggipfel und hervortretende Gebirgsstrukturen (nach BAS 1993, IfAG/AWI 1994, BKG 1998) sind durch dünne schwarze Linien hervorgehoben. Die Meeresbodentopographie lässt sich nicht anhand der Flugmessdaten bestimmen.

Thyssen (1988), the new map displayed in Figure 7 shows the bedrock relief in western Neuschwabenland in much more detail. But there are also significant differences between both maps. While Hoppe & Thyssen (1988) found the ice-sheet base in the western and central parts of Ritscherflya to be mainly structured by various elongated ridges and depressions extending from west towards east or northeast, the new bedrock-elevation model yields a more complex pattern of individual large-scale depressions and subglacial mountainous regions. In particular, the mentioned general subdivision of Ritscherflya into three parts is only discernible in the improved maps of this study.

CONCLUSIONS

The combined processing of the aero-geophysical measurements from the field seasons 1985/86 and 1988/89 yield improved and more detailed maps of the ice-sheet geometry in western Neuschwabenland. In particular, the maps revealed new insights in the ice-thickness distribution and the morphological setting there. Although the accompanying digital geometric models are based on irregularly distributed measuring points and are probably inaccurate in some parts, these models additionally represent essential input data for further investigations such as numerical modelling studies or geological and tectonic interpretations. Of special interest might be quantitative investigations on the sensitivity of the mass balance of the outlet glacier Jutulstraumen to (climatic induced) changes in the accumulation rate in the catchment area or in the lateral extension and the thickness distribution of the adjacent ice shelf Jelbartisen. Since the boundaries of Jutulstraumen coincide with distinct graben-like depressions in the bedrock topography, even small variations in the horizontal mass flux might cause significant changes in the position of the grounding line. This, in turn, would probably have a far-reaching influence on the ice dynamics, the flow regime, and the ice-sheet geometry of the northeastern part of western Neuschwabenland.

ACKNOWLEDGEMENTS

The aerial surveys of 1988/89 were supported by the Deutsche Forschungsgemeinschaft under grant TH168/20-1. We are grateful to F. Thyssen, who was the initiator of this project, to M. Jonas, who was involved in the field measurements besides the co-author, and to the labs of the Institut für Geophysik der Universität Münster for constructing the RES system. The processing of the recorded data sets was carried out within the DYPAG (Dynamic Processes in Antarctic Geosystems) project, funded by the Bundesministerium für Bildung, Wissenschaft, Forschung und Technologie der Bundesrepublik Deutschland, contract 03PL016A. Thanks are due to J. Sievers, H. Bennat, and B. Heidrich of the Bundesamt für Kartographie und Geodäsie, Frankfurt a. Main, for providing the satellite-image mosaic of western Neuschwabenland and the adjacent ice-shelf and ice-sheet areas. We would also like to thank J.L. Bamber for the provision of the digital elevation model describing the surface topography of Antarctica. This paper was improved as a result of the comments of two anonymous reviewers.

References

Bamber, J.L. & Huybrechts, P. (1996): Geometric boundary conditions for modelling the velocity field of the Antarctic ice sheet.- Ann. Glaciol. 23: 364-373.

BAS (1993): SCAR Antarctic digital database.- Vers. 1.0, British Antarctic Survey, Cambridge.

BKG (1998): Satellite image map Dronning Maud Land 1:2000000.- Draft Vers. 4.2 (Nov. 1998), Bundesamt für Kartographie und Geodäsie, Frankfurt am Main.

Blindow, N. (1986): Bestimmung der Mächtigkeit und des inneren Aufbaus von Schelfeis und temperierten Gletschern mit dem hochauflösenden elektromagnetischen Reflexionsverfahren.- Unpubl. Dissertation, Westfälische Wilhelms-Universität Münster, 166 pp.

Drewry, D.J. (1983): Antarctica: glaciological and geophysical folio.- Scott Polar Research Institute, Cambridge.

Hoppe, H. & Thyssen, F. (1988): Ice thickness and bedrock elevation in western Neuschwabenland and Berkner Island, Antarctica.- Ann. Glaciol. 11: 42-45.

IfAG (1993): Satellite image map 1:1 000 000 SS 28-30 Ritscherhochland, Antarctica.- 3rd ed., Institut für Angewandte Geodäsie, Frankfurt a. Main.

IfAG/AWI (1994): Digital topographic Antarctic data base.- Vers. 1.94 (G), Institut für Angewandte Geodäsie, Frankfurt a. Main, and Alfred-Wegener-Institute for Polar and Marine Research, Bremerhaven.

Sandhäger, H. & Blindow, N. (2000): Surface elevation, ice thickness, and subglacial-bedrock topography of Ekström Ice Shelf (Antarctica) and its catchment area.- Ann. Glaciol. 30, (in press)

Thyssen, F. & Grosfeld, K. (1988): Ekström Ice Shelf, Antarctica.- Ann. Glaciol. 11: 180-183.